Nucleon elastic form factors and local duality

R. Ent
Thomas Jefferson National Accelerator Facility, Newport News, Virginia 23606

C. E. Keppel
Thomas Jefferson National Accelerator Facility, Newport News, Virginia 23606
and Hampton University, Hampton, Virginia

I. Niculescu
Hampton University, Hampton, Virginia

(Received 14 May 1999; published 7 September 2000)

Using a newly obtained sample of inclusive electron-proton scattering data in the nucleon resonance region we have extracted the proton magnetic form factor, utilizing the quark-hadron duality concept. The extraction is in good agreement with direct measurements. Similarly, utilizing quark-hadron duality, a relation can be derived between the ratio of longitudinal to transverse deep inelastic electron-proton scattering cross sections and the ratio of the electric to magnetic proton elastic form factors. Again, the extracted ratio agrees reasonably with the existing world data. This agreement is a first experimental verification of duality in the longitudinal channel, and suggests that effects of higher-twist operators are suppressed on average in both the longitudinal and transverse electron-nucleon scattering processes.

PACS number(s): 13.40.Gp, 12.38.Qk

Nearly three decades ago, Bloom and Gilman observed that the prominent resonance enhancement region observed in inclusive electron-proton scattering averages to, and tracks with changing momentum transfer, the smooth scaling curve of the deep inelastic structure function, if expressed in terms of a scaling variable connecting the two different kinematic regimes [1,2]. This relationship between resonance electroproduction and the scaling behavior observed in deep inelastic scattering, termed local duality, suggests a common origin for both phenomena. Duality shows that the single-quark scattering process determines the scale of the reaction, even in the nucleon resonance region. Additional interactions between the struck quark and the spectator quarks (higher-twist effects) will nonetheless occur in this region, inducing much or most of the final state to produce a given resonance. However, if one averages over a reasonably wide region of kinematics, these additional interactions appear to cancel out and the reaction process still mimics the single-quark scattering process. A quantitative quantum chromodynamics (QCD) analysis of this empirical observation was given by De Rujula, Georgi, and Politzer [3,4]. They showed that local duality holds if averaged over a large kinematic region, as the higher-twist effects are not large. Such QCD explanations of quark-hadron duality apply as well to the longitudinal structure function as the transverse [5].

Experimentally, higher-twist terms in the deep inelastic F_2 data have been found to be small for Bjorken $x<0.40$ [6]. Recently, a reanalysis of deep inelastic F_2 data led to modified parton distribution functions [7]. Starting from these modified distribution functions the authors conclude that, in next-to-leading order (NLO) analyses, only minor higher-twist effects are needed to describe the deep inelastic F_2 data and $R=\sigma_L/\sigma_T$ (the ratio of longitudinal to transverse deep inelastic lepton-nucleon scattering), up to large Bjorken x and down to four-momentum transfer squared $Q^2=1$ $(\mathrm{GeV}/c)^2$. Furthermore, when this analysis of R was repeated in next-to-next-to-leading order (NNLO), the higher-twist contributions were found to be even smaller [7]. In this analysis, the Georgi-Politzer calculation [8] was used to take target-mass corrections into account. These target-mass corrections, in terms of the Nachtmann variable $\xi=2x/(1+\sqrt{1+4M^2x^2/Q^2})$ [9], where M is the proton mass, are necessary as the quarks cannot be treated as massless partons for low to moderate momentum transfers.

Local duality between resonance electroproduction and deep inelastic scattering has been recently shown to hold surprisingly well down to momentum transfers squared, Q^2, as low as 1.0 $(\mathrm{GeV}/c)^2$ [10]. It was shown that, if integrating over local nucleon resonance regions, the average strength in this region and the deep inelastic scaling curves agree to better than 10%, down to $Q^2=1.0$ $(\mathrm{GeV}/c)^2$. Even more dramatic, a scaling curve can be established representing the average of *all* proton resonance data in the region $M^2\leqslant W^2<4$ GeV^2 and $Q^2<5$ $(\mathrm{GeV}/c)^2$, and the data at various values of Q^2 and W^2 oscillate around this averaged scaling curve. To illustrate, we show in Fig. 1 three sample $^1\mathrm{H}(e,e')$ proton resonance spectra in combination with this averaged scaling curve. Consistent with Bloom and Gilman's observation, the resonance enhancements at different Q^2 appear at different ξ, but always on the same scaling curve. The dashed curve represents a global fit to the world's deep inelastic data [11] for a fixed $Q^2=10$ $(\mathrm{GeV}/c)^2$. The solid curve represents the resonance-averaged scaling curve. Resonance spectra with as low a Q^2 as 0.1 $(\mathrm{GeV}/c)^2$ and as high a Q^2 as 10 $(\mathrm{GeV}/c)^2$ all seem to oscillate around this global scaling curve. We want the reader to be aware that this is non-trivial; e.g., at $\xi=0.5$ resonance excitations between $Q^2=1$ and $Q^2=3$ $(\mathrm{GeV}/c)^2$ contribute.

The two observations mentioned; i.e., higher-twist contributions to R in deep inelastic scattering data are small up to

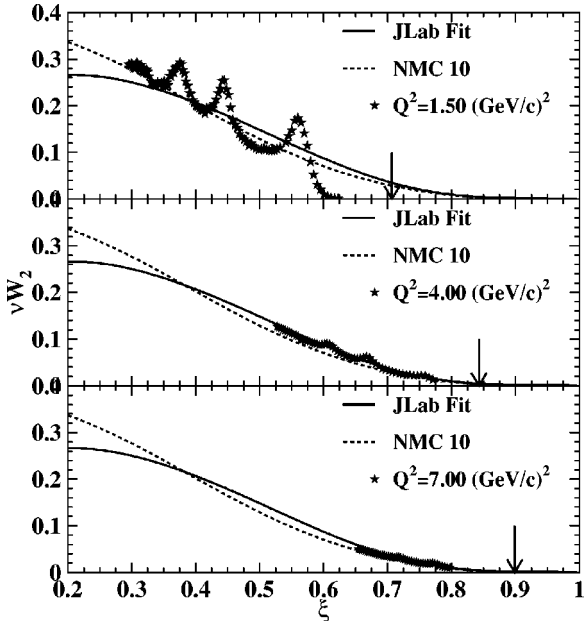

FIG. 1. Sample hydrogen F_2 structure function spectra obtained at $Q^2 \sim 1.5$, 4, and 7 $(\mathrm{GeV}/c)^2$ and plotted as a function of the Nachtmann scaling variable ξ. Arrows indicate elastic kinematics. The dashed line represents the NMC fit [11] of deep inelastic structure function data at $Q^2 = 10$ $(\mathrm{GeV}/c)^2$. The solid line indicates the scaling curve obtained by averaging the world's electron-proton resonance excitation data.

large x and down to $Q^2 = 1.0$ $(\mathrm{GeV}/c)^2$ and local duality appears to work to better than 10% down to $Q^2 = 1.0$ $(\mathrm{GeV}/c)^2$ beg the question as to how well the proton elastic electric and magnetic form factors can be determined from duality arguments.

First, we give the functional form for the resonance-averaged F_2 scaling curve we used (the solid curve in Fig. 1)

$$F_2 = \xi^{0.870}(1-\xi)^{0.006}[0.005 - 0.058(1-\xi) - 0.017(1-\xi)^2 + 2.469(1-\xi)^3 - 0.240(1-\xi)^4]. \quad (1)$$

We believe the systematic uncertainty in this functional form to be similar to the systematic uncertainty of 3.5% in the proton resonance data [12–14]. Following Georgi and Politzer [8,15] the proton elastic magnetic form factor can be derived from F_2:

$$G_M{}^2 = \frac{1+4M^2/\mu^2Q^2}{1+4M^2/Q^2}\,\frac{2-\xi_p}{\xi_p{}^2}\int_{\xi_{thr}}^{1} F_2 d\xi. \quad (2)$$

Here, ξ_p corresponds to the ξ for elastic scattering ($x=1$), ξ_{thr} to the ξ corresponding to pion threshold, and μ is the proton anomalous magnetic moment. Figure 2 depicts the proton magnetic form factor, G_M, extracted using the NMC (open circles) [11] and JLab (solid circles) scaling curves integrated over the *entire* range in ξ, i.e. from $\xi=1$ to the deep inelastic. The integral obtained from the resonance data (which stops at ξ_{thr} for pion threshold rather than at $\xi=1$) is then subtracted from the scaling integrals. The magnetic

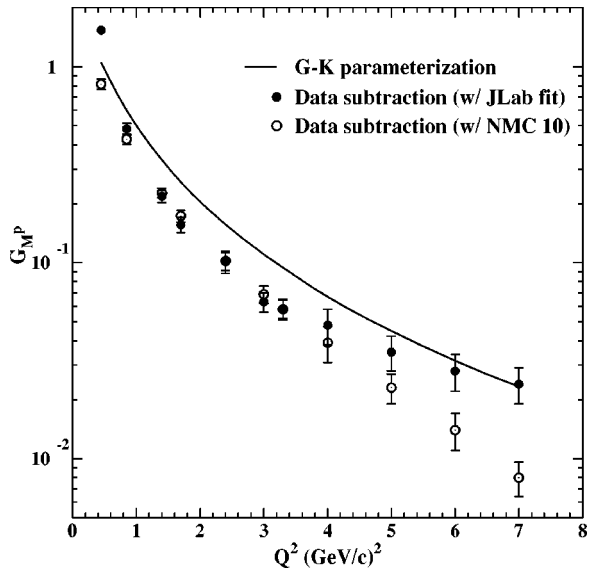

FIG. 2. The proton magnetic form factor extracted from the inelastic data using duality assumptions as described in the text. The extracted data are compared to the model curve of [16], which agrees with the global data set.

form factor is then extracted from the remaining integrated strength. In both cases, the extracted integrals are in remarkable agreement with the Gari-Krümpelmann model (solid line) [16]. The latter follows, in the momentum transfer range of interest, the world's magnetic form factor data quite well. For the JLab scaling curve worst case, we reproduce the proton magnetic form factor to within 30% of the accepted value, down to Q^2 of 0.2 $(\mathrm{GeV}/c)^2$ and up to Q^2 of 7 $(\mathrm{GeV}/c)^2$.

After having compared the world's data on the proton elastic magnetic form factor with a duality-based extraction from purely inelastic data, we will in the remainder of this paper concentrate on the ratio of the proton elastic electric to magnetic form factors. Since R in the nucleon resonance region is presently only known at the $\pm 100\%$ level in the nucleon resonance region above $Q^2 \approx 1$ $(\mathrm{GeV}/c)^2$ [17], we will in this case only use R from deep inelastic data. However, one has to bear in mind that the duality-extracted values for G_M were closer to the world's data for the resonance-averaged scaling curve than for the deep inelastic fit, and hopefully, likewise, a better extraction of the proton elastic form factor ratio could follow from a resonance-averaged measurement of R. The definitions of the electric and magnetic form factor (G_E and G_M, respectively) lead to a straightforward relation between their ratio G_E/G_M and R [8,18]:

$$\frac{\mu G_E}{G_M} = \frac{\mu Q}{2M}\sqrt{\frac{\int d\xi \sigma_L}{\int d\xi \sigma_T}}, \quad (3)$$

where we have included μ on both sides of the equation. We calculate σ_L as $R \times \sigma_T$, and calculate σ_T from the resonance-averaged scaling curve for F_2 using

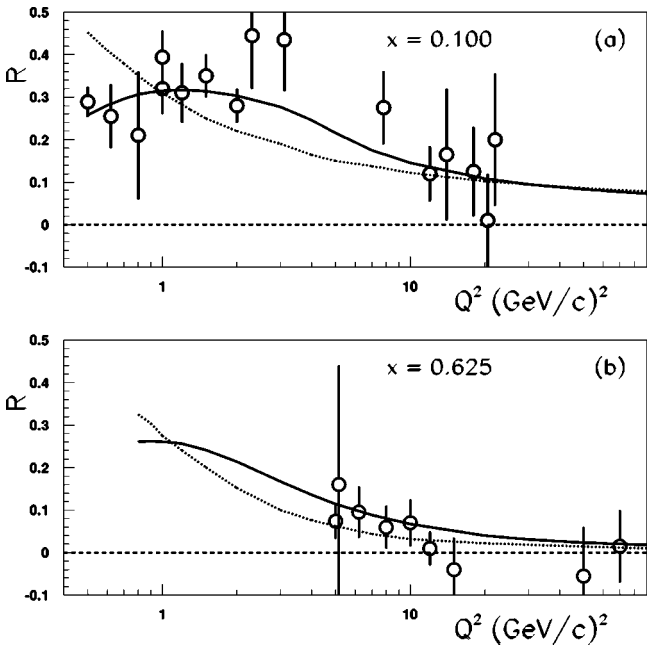

FIG. 3. Experimental values for R at $x=0.100$ (a) and $x=0.625$ (b). The data (circles) have been extracted from Ref. [20]. The solid line indicates the global fit to the world's data of R from Ref. [19]. The dotted line is the result from a QCD calculation including target-mass effects following Georgi and Politzer [8,19,21].

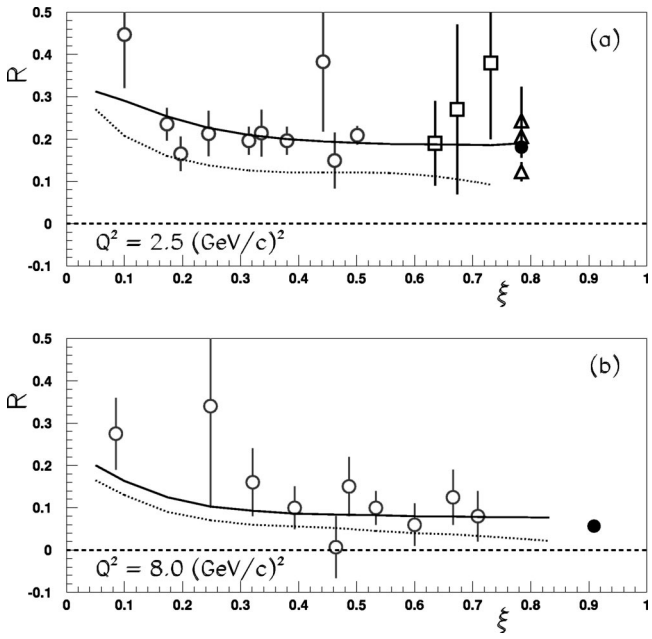

FIG. 4. Experimental values for R as a function of ξ, at fixed $Q^2=2.5$ (GeV/c)^2 (a) and $Q^2=8.0$ (GeV/c)^2 (b). Open circles are data obtained in the deep inelastic scattering region [19,20]. Squares are from data averaged over the full resonance region extracted from Ref. [22]. Triangles are elastic data from Refs. [24,25]. The solid lines indicate the global fit to the world's data of R from Refs. [19]. The dotted line is the result from a QCD calculation including target-mass effects following Georgi and Politzer [8]. The solid circles indicate the expected value at $x=1$ for elastic form factor scaling.

$$\sigma_T = F_2\left[\frac{4\pi^2\alpha}{\nu}\,\frac{2M}{W^2-M^2}\,\frac{1+\nu^2/Q^2}{1+R}\right], \tag{4}$$

where ν is the electron energy loss, and α is the fine-structure constant.

The integrals are performed over the region between ξ corresponding to pion threshold and $\xi=1.0$. Note that this implies that the lower integration limit varies as a function of Q^2. For R we choose two different forms, one given by the best fit to the world's deep inelastic data [19,20], the other as derived from a QCD calculation including target-mass corrections, using parton distribution functions as input [8,19]. Although the latter calculation is old, it will not affect our conclusions later on. The main purpose of using this QCD calculation is didactical, to show the reader how a different form for R affects the extraction of the ratio G_E/G_M. Also note that the kinematic effects due to target mass dominate at small Q^2 and large x, the region where we can relate the deep inelastic R data to the elastic form factors by duality.

In Fig. 3 we show a sample of the world's data on R from deep inelastic scattering. The data have been extracted from Refs. [19–21]. The data at $x=0.100$ extend down to low Q^2, approximately 0.5 (GeV/c)^2, whereas the data at $x=0.625$ initiate at $Q^2\approx 4$ (GeV/c)^2. Note that equating the elastic data in terms of Nachtmann ξ to the deep inelastic data at the same ξ corresponds to, for example, comparing deep inelastic data at [$Q^2=5$ (GeV/c)^2, $W^2=4$ (GeV)^2] to elastic data at [$Q^2=0.7$ (GeV/c)^2, $W^2=M^2$], where W is the invariant mass of the hadronic system. Thus, in order to perform the duality-based derivation of $\mu G_E/G_M$ from R, we need to extend the models and calculations for R into a region where they are not constrained by measurements. In principle a similar extrapolation has to be made for the local duality witnessed in resonance electroproduction data and deep inelastic data [1,2], but as the world's data on F_2 at small to intermediate Q^2 and intermediate to large x show predominantly an x dependence, and less of a Q^2 dependence, this is less of an issue. In contrast, the world's data for R in these regions show more of a Q^2 dependence, and hardly an x dependence [19–21]. This can be seen from Fig. 3 in that the fit [19] to the world's data on R (solid curve) varies little between $x=0.100$ (Fig. 3a) and $x=0.625$ (Fig. 3b).

We expand on this in Fig. 4, where we show a sample of the world's data on R as a function of ξ, now at *fixed* values of $Q^2=2.5$ (GeV/c)^2 (Fig. 4a) and of $Q^2=8.0$ (GeV/c)^2 (Fig. 4b). The solid curve is again the fit to the world's data on R. The open circles are data obtained in the deep inelastic scattering region [19–21]. The squares are data in the nucleon resonance region, *averaged* over the full region [22]. The triangles are elastic data from Refs. [23–25]. The R data show a smooth ξ dependence, regardless whether the data are from the deep inelastic, the resonance, or the elastic region. To first order this confirms the local duality picture in the ratio R. The solid circles indicate the expected values for R in the elastic case assuming form factor scaling, i.e. assuming that the charge and magnetic moment distributions have the same spatial dependence. This underlines the fact that the

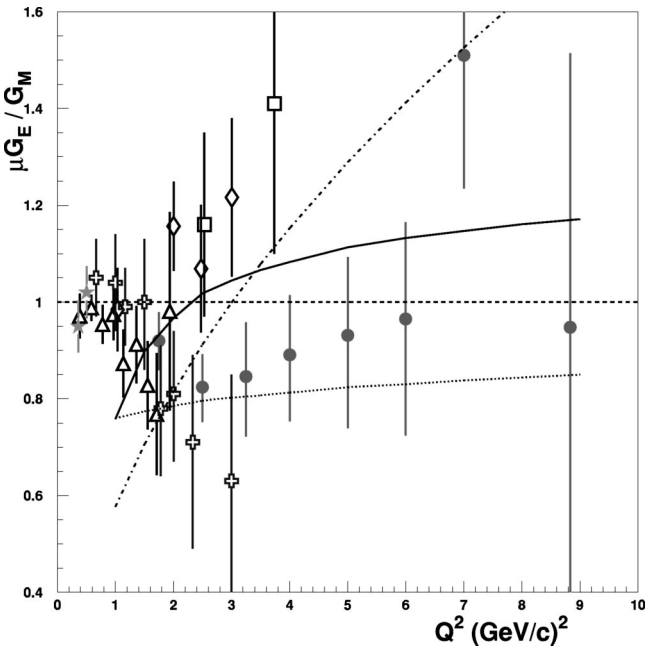

FIG. 5. The derived values for the ratio of the proton electric and magnetic form factor using local duality and (solid curve) the fit to the world's data on the ratio of longitudinal to transverse deep inelastic scattering [19], (dotted curve) a QCD calculation including target-mass corrections following Georgi and Politzer [8], and (dot-dashed curve) a constant value of $R=0.15$. The experimental data are from Ref. [26] (pluses), Ref. [27] (triangles), Ref. [23] (squares), Ref. [24] (diamonds), Ref. [25] (circles), and Ref. [29] (stars).

fit [19] to the world's *deep inelastic* data on R smoothly links to available elastic data. Note, however, that the fit does not appear to go through the form factor scaling points at $x=1$ at Q^2 below 1 $(\mathrm{GeV}/c)^2$ [19,20].

To estimate model dependencies in extrapolations from measured kinematics in x and Q^2 of the deep inelastic data, we also used R calculated following the formalism of Georgi and Politzer [8,19,21]. Here, starting with input parton distribution functions, target mass effects are included in the framework of the operator product expansion and QCD moment analysis. The results of such a calculation are indicated by the dotted curves in Figs. 3 and 4. These calculations have no inherent elastic constraints and do not seem to go through the form factor scaling points at $x=1$ (in terms of ξ, the elastic scaling points are at $\xi=0.78$ and 0.91, respectively). The solid and dotted curves vary drastically; however, they both show a rising trend in R towards smaller Q^2.

In Fig. 5, we show the world's data on the ratio $\mu G_E/G_M$ of proton elastic form factor data. Most of these data [23–27] have been determined using the conventional Rosenbluth separation technique [28], and may be prone to large systematic uncertainties. This is evident in the large scatter of the data (note that the uncertainties for the data points from Ref. [25] include the published systematic uncertainties). More recently, a different technique has been used to reduce the systematic uncertainties by measuring the $^1\mathrm{H}(\vec{e},e'\vec{p})$ polarization transfer reaction [29,30]. In this method a direct ratio of polarization transfer observables is measured, directly proportional to the ratio $\mu G_E/G_M$, precluding the necessity to have two kinematically independent points as needed for a Rosenbluth separation. The dashed curve (constant at unity) in Fig. 5 indicates the expected behavior of $\mu G_E/G_M$ according to form factor scaling.

The remaining curves utilize the duality approach. The solid curve in Fig. 5 is the extraction of the elastic form factor from deep inelastic data using the fit [19], and the dotted curve is the extraction using the QCD (including target mass effects) calculation following the formalism of Georgi and Politzer [8,19,21]. Above we indicated observations [7,10] leading us to believe that higher-twist effects (apart from target-mass corrections) are reduced at $Q^2>1$ $(\mathrm{GeV}/c)^2$, which is where we start our duality-motivated form factor extractions. The difference between using R from the fit to the world's data and the QCD including target mass effects calculation (see Fig. 3b and Fig. 4) mimics the difference in the extraction of $\mu G_E/G_M$ using duality arguments. The calculations indicate only a slight Q^2 dependence, which is caused by countering effects of the linear dependence on Q in Eq. (3) and the Q dependence of the integral ratio. The latter has two dependences on Q, one in the integration area as the ξ belonging to pion threshold increases as a function of Q^2, thus decreasing the integration area, and one in the Q dependence of R. Apparently the absolute value of R at low Q^2 is of less relevance. We have included in Fig. 5 a dot-dashed curve assuming a *fixed* R of 0.15, which shows that obtaining the Q^2 dependence of this quantity by duality-extracted predictions for the ratio of elastic form factors is a non-trivial property of the nucleon, requiring the Q^2 dependence of R. The agreement between the two (non-constant R) duality-based extractions and the world's data on $\mu G_M/G_E$ is in our opinion amazingly good (we stress that no normalization was necessary). This result is non-trivial: even if higher-twist contributions cancel to a large extent in F_2 if one averages over the full nucleon resonance region, even down to very low Q^2, it is not clear at all that higher-twist similarly will cancel in the longitudinal inclusive electron-nucleon scattering response. Especially, we can only extract the elastic form factors if duality also works in a very localized region in ξ. If higher-twist terms would not cancel on average in the longitudinal response, the duality-based curves in Fig. 5 could easily be off by an order of magnitude.

The above extraction will be even more constrained when more data on R in the nucleon resonance region will become available. Again, using (local) duality arguments, this would render experimental values of R closer to the kinematic region where we use them for the extraction of $\mu G_E/G_M$. As mentioned above, the magnetic form factor was extracted from purely inelastic data using duality arguments to better than 30% in a large Q^2 range. This may indicate a similar absolute uncertainty on this duality-based extraction of $\mu G_M/G_E$. Still, we feel this result may be interpreted as a strong signature that higher-twist effects are also reduced in the longitudinal response of the electron-proton scattering process, if the data are averaged over a reasonably large kinematic region.

In summary, we have extracted the proton elastic magnetic form factor and the ratio of the proton elastic electric and magnetic form factors from purely deep inelastic data using quark-hadron duality arguments. The results agree reasonably with experimental data, suggesting that higher-twist contributions are suppressed in both the transverse and the longitudinal parts of the electron-proton scattering process, if averaged over an extended kinematic region. This is an experimental indication that duality should hold on average in the longitudinal channel, as has been observed before in the transverse; i.e., both the longitudinal and transverse parts of electron-proton scattering seem to resemble on average a single-quark scattering process.

This work was supported in part by the U.S. National Science Foundation under Grant No. HRD-9633750 (Hampton). C.E.K. acknowledges the support of the NSF Early Faculty Career Development Program.

[1] E.D. Bloom and F.J. Gilman, Phys. Rev. D **4**, 2901 (1970).
[2] E.D. Bloom and F.J. Gilman, Phys. Rev. Lett. **25**, 1140 (1970).
[3] A. DeRujula, H. Georgi, and H.D. Politzer, Phys. Lett. **64B**, 428 (1976).
[4] A. DeRujula, H. Georgi, and H.D. Politzer, Ann. Phys. (N.Y.) **103**, 315 (1977).
[5] C. Carlson and N. Mukhopadhyay, Phys. Rev. D **41**, 2343 (1990).
[6] M. Virchaux and A. Milsztajn, Phys. Lett. B **274**, 221 (1992).
[7] U.K. Yang and A. Bodek, Phys. Rev. Lett. **82**, 2467 (1999).
[8] H. Georgi and H.D. Politzer, Phys. Rev. D **14**, 1829 (1976).
[9] O. Nachtmann, Nucl. Phys. **B63**, 237 (1975).
[10] I. Niculescu *et al.*, Phys. Rev. Lett. **85**, 1186 (2000).
[11] M. Arneodo *et al.*, Phys. Lett. B **364**, 107 (1995).
[12] I. Niculescu, Ph.D. thesis, Hampton University, 1999.
[13] D. Abbott *et al.*, Phys. Rev. Lett. **80**, 5072 (1998).
[14] G. Niculescu *et al.*, Phys. Rev. Lett. **81**, 1805 (1998).
[15] S. Simula, G. Ricco, M. Anghinolfi, M. Ripani, and M. Taiuto, Few-Body Syst., Suppl. **10**, 423 (1999); S. Simula (private communications).
[16] M. Gari and W. Krümpelmann, Phys. Lett. **141B**, 295 (1984).
[17] An experiment to measure R in the nucleon resonance region (E94-110, spokesperson C.E. Keppel) just finished data taking at JLab.
[18] F.E. Close, *An Introduction to Quarks and Partons* (Academic, Great Britain, 1979).
[19] L.W. Whitlow *et al.*, Phys. Lett. B **250**, 193 (1990); L.W. Whitlow, Ph.D. thesis, American University, 1990.
[20] L. Tao *et al.*, Z. Phys. C **70**, 387 (1996); L. Tao, Ph.D. thesis, American University, 1994.
[21] S. Dasu *et al.*, Phys. Rev. D **49**, 5641 (1994).
[22] C.E. Keppel, Ph.D. thesis, American University, 1994.
[23] J. Litt *et al.*, Phys. Lett. **31B**, 40 (1970).
[24] R.C. Walker *et al.*, Phys. Lett. B **224**, 353 (1989); **240**, 522 (1990); Phys. Rev. D **49**, 5671 (1994).
[25] L. Andivahis *et al.*, Phys. Rev. D **50**, 5491 (1994).
[26] W. Bartel *et al.*, Nucl. Phys. **B58**, 429 (1973).
[27] Ch. Berger *et al.*, Phys. Lett. **35B**, 87 (1971).
[28] M.N. Rosenbluth, Phys. Rev. **79**, 615 (1950).
[29] B.D. Milbrath *et al.*, Phys. Rev. Lett. **80**, 452 (1998).
[30] Jefferson Lab Experiment E93-027, analysis in progress.